Response to Referee #2

(Referee comments: https://doi.org/10.5194/egusphere-2023-2916-RC2)
Manuscript: Yessimbet, K., Steiner, A. K., Ladstädter, F., and Ossó, A.: Observational perspective on SSWs and blocking from EP fluxes, EGUsphere [preprint], https://doi.org/10.5194/egusphere-2023-2916, 2024.

The structure and content of the referee's comments are duplicated below. The authors' responses are in bold. Line numbers used in our responses refer to the original ACP Discussions paper. Text updates in the revised manuscript are in grey.

Summary:

This work examines the structure, origin, and tropospheric influence of eight major SSW events between 2007 and 2019. All analysis is based on GNSS RO derived temperature soundings. The data are horizontally gridded to provide the geostrophic winds needed to derive factors that characterized SSW events such as EP flux and EP flux divergence. Displacement (type 1), splitting, and mixed SSW events (type 2) are compared and contrasted. The study focuses on the relation between the lower stratosphere (100 - 10 hPa), the troposphere, and tropospheric blocking during the evolution of SSW events. Results showed that GNSS RO observations are capable of capturing the main features of the SSW events. Examination of wave reflecting and absorbing SSW events highlighted the relatively short duration of the wind reversal as well as the formation of the North Pacific blocking pattern during wave reflecting events. Results also showed that the behavior of the enhanced upward EP flux prior to the SSW events differed between the two types of warming events. Furthermore, the TIL was found to depend on the magnitude of the SSW near the tropopause.

We thank the reviewer for reviewing our manuscript. We also thank the reviewer for all the valuable comments and suggestions and for emphasizing the strengths and weaknesses of the work.

Strengths:

The paper relates a two-dimensional, zonally averaged, dynamical analysis of SSW events to the evolution of tropospheric blocking events, providing an analysis of connections between changes in both the stratosphere and the troposphere. The detailed examination of the two main patterns identified provided a useful and engaging approach to characterizing all the warming events in the study. The dependence of the TIL on the structure of the warming event was an intriguing result.

Weakness:

1) The use of geostrophically derived winds in the stratosphere can lead to errors in the EP flux calculation. As shown in Boville (1987) the stratospheric heat flux and momentum flux errors can be as large as 40%. For example, Fig. 1 arrows at 60N and 10 hPa are nearly vertical, differing

from the NH winter climatology shown in Butchart (2022, Fig. 4a). While the citations in the text claim reasonable errors when using the geostrophic approximation, some comparison with corresponding reanalysis results should be shown to justify reliance on the geostrophic approximation, especially for the stratospheric fields.

Butchart, N.: The stratosphere: a review of the dynamics and variability, Weather Clim. Dynam., 3, 1237–1272, https://doi.org/10.5194/wcd-3-1237-2022, 2022.

Boville, B. A.: The validity of the geostrophic approximation in the winter stratosphere and troposphere, J. Atmos. Sci.,44,pp 443-457, 1987.

Thank you for raising this important aspect. During our analysis, we compared our RO-based geostrophic parameters with non-geostrophic parameters based on reanalyses (ERA5 and NCEP). The primary information is obtained from two zonally averaged parameters such as zonal-mean zonal wind ($\bar{u}$), and eddy meridional heat flux ($\overline{v'T'}$). Figures S2,3 (also here R2.1,2.2) provide a comparison of these parameters and show consistency between RO and ERA5 both in the stratosphere and upper troposphere, confirming the reliability of RO-based dynamics.
Additionally, Leroy et al (2007), who computed quasi-geostrophic EP flux from RO, demonstrated that the vertical component of EP flux has a difference of only about 5-10% with the NCEP reanalysis while the horizontal component of the momentum flux has a larger difference of about 30-40%. In our work, we mainly focus on the vertical component of the EP flux because it is the vertical component that controls the stratospheric adiabatic circulation, and thus is the main informative parameter.
Also, our study uses geostrophic winds based on Scherllin-Pirscher et al. (2014), who showed that all major wind features are captured, and compared to atmospheric analyses, winds are only about 2 m/s weaker except near the subtropical jet where the difference is larger (up to 10 m/s).
We added the following information in the revised manuscript to the data description:
Geostrophic wind fields can be derived from RO geopotential height fields (Scherllin-Pirscher et al., 2014; 2017). RO geostrophic wind and gradient wind fields were found to capture all main wind features in our study. Compared to atmospheric analyses, wind differences are generally small (2 m/s) except near the subtropical jet (up to 10 m/s). There, RO winds underestimate actual winds due to the geostrophic and gradient wind approximations while RO retrieval errors have negligible effects (Scherllin-Pirscher et al., 2014).

We added also some information about the comparison of parameters between RO and ERA5 in the manuscript at Line 123:
In our analysis, we also made a comparison of key parameters between RO and reanalyses (e.g., ERA5), such as the zonally averaged parameters, zonal-mean zonal wind and $\overline{v'T'}$

(Figures S2 and S3), confirming the consistency and the reliability of the RO-based dynamics.

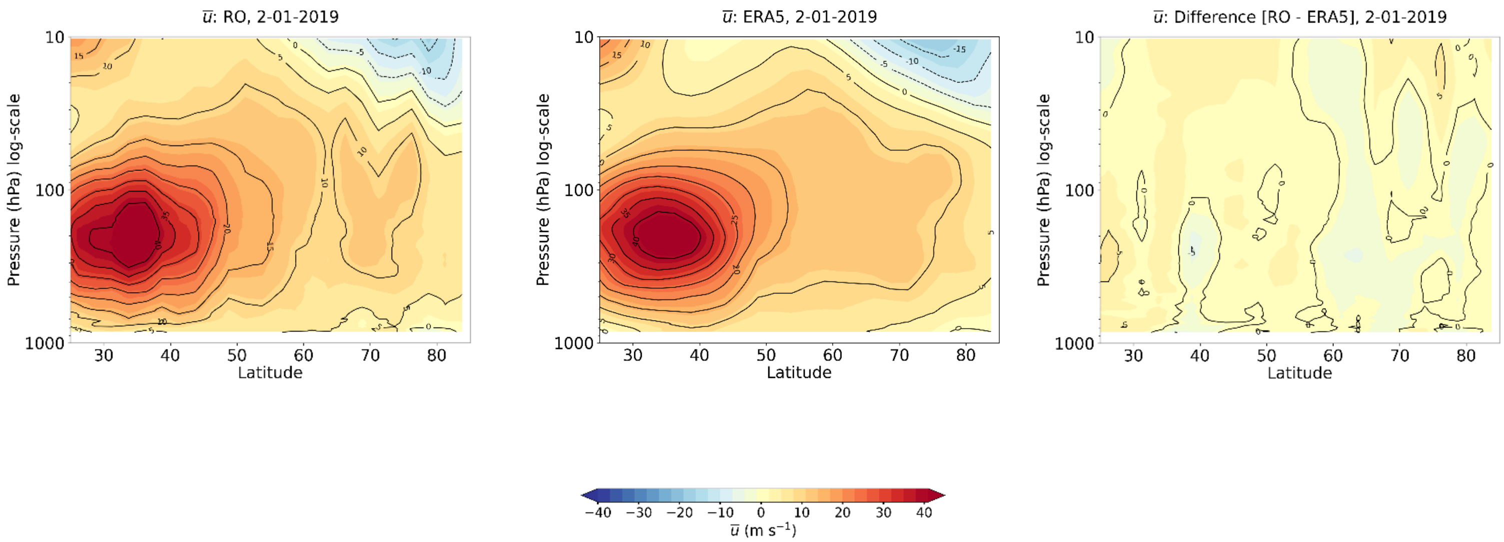

Figure R2.1. Zonal-mean zonal wind computed from RO (geostrophic wind; left) and ERA5 (real wind; right) and their difference for an exemplary day.

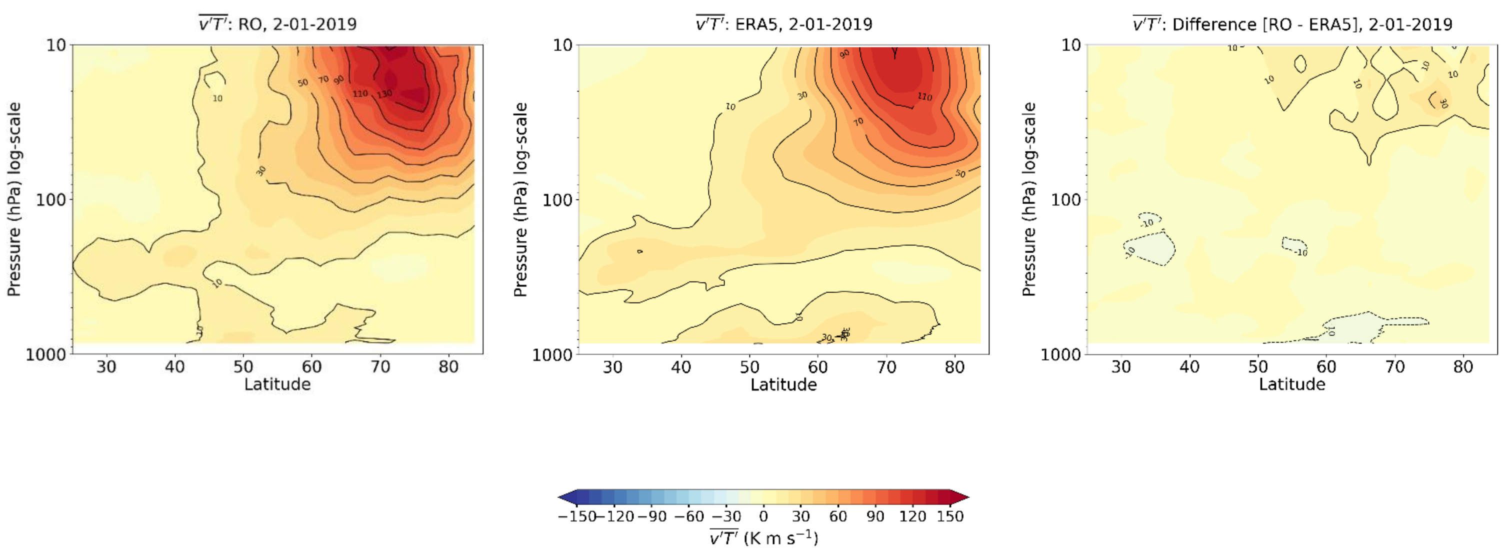

Figure R2.2. Eddy meridional heat flux computed from RO (using geostrophic meridional wind; left) and ERA5 (using real meridional wind; right) and their difference for an exemplary day.

Concerning the EP flux vectors, which in our manuscript (e.g., Fig.1) appear almost vertical in the stratosphere, we re-checked the calculation of the EP flux and found that the choice of the scaling of the EP flux vectors was the problem. In the initial manuscript version, we scaled the EP flux vector by the $\sqrt{1000/pressure}$, while Butchart (2022) did not use this scale factor. Once we remove this additional scale factor, the vectors look more similar to Fig.4 in Butchart (2022) (see Figure below). Regarding this scale factor, Jucker et al (2021) state that this commonly used scale factor should be used with caution and may not always be useful as it does not have any physical meaning. We decided to remove this scale factor and re-plotted all figures.

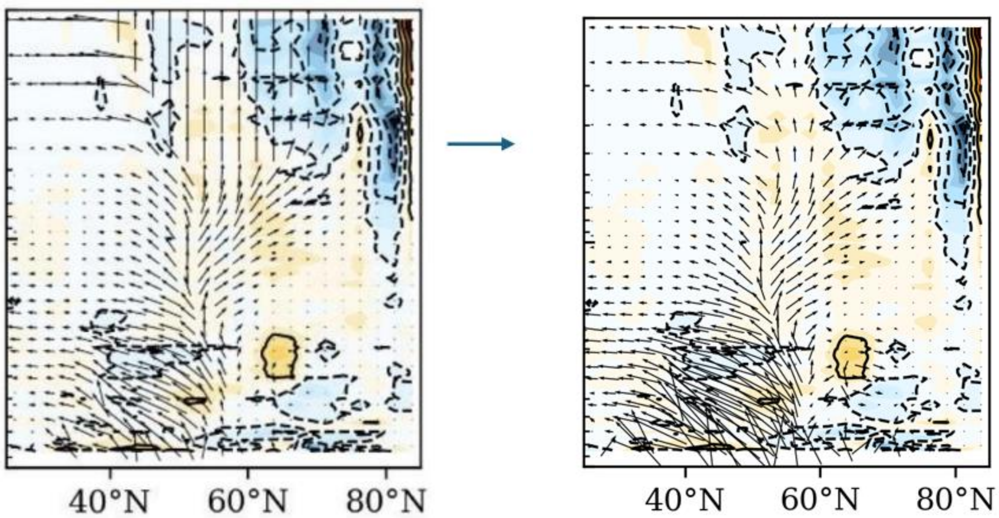

Figure R2.3.: Meridional cross section of EP flux vectors, Fig. 2c initial manuscript (left) and revised manuscript (right).

2) It is not clear how the high vertical resolution of the GNSS RO observations contributed to the results as the vertical grid used seemed similar to current model and reanalyses. Is this work mainly a feasibility study for future work based on GNSS RO observations? More explanation can be done here.

Sorry for having caused confusion. The main objective of our study was to get a better understanding on the vertical coupling between the troposphere and stratosphere and the relationship between SSWs and blocking events by investigating the vertical structure of planetary wave propagation, static stability, geometry of the polar vortex, and the occurrence of blocking events from an observational viewpoint. We therefore position this study as an extension of observational knowledge of stratosphere-troposphere dynamics and SSW events.

The feasibility of GNSS RO has already been investigated by several studies as stated and cited in the introduction section of the manuscript (see the references below). However, we have also made further comparisons with reanalyses, confirming the consistency of the RO-based dynamics (see response to comment 1).
In addition, we compared the Brunt Väisälä frequency (Fig. S4/R3.4) which shows high consistency in terms of main patterns and magnitude between RO and ERA5. Small differences (of around 10%) in N^2 are observed mainly in the tropopause region between 200 hPa and 300 hPa and in the stratosphere.
It should be noted that we chose to compare with ERA5 because it is arguably the most advanced and commonly used reanalysis product, however, ERA5 assimilates RO data. RO data has a high vertical resolution, while the daily gridded field is smoothed in the horizontal and over time due to weighted averaging. Therefore, it is not straightforward to interpret the differences in detail.
However, for our study we decided to take the observational perspective and chose to use GNSS RO observations for the analyses as the dataset resolves the relevant features to provide information on the stratosphere–troposphere coupling.

For better clarity we revised the manuscript text, specifically the first and last paragraph in the discussion section, which now read:
The main objective of this study was to characterize the synoptic and dynamic conditions of SSWs and to investigate the link to blocking events from an observational perspective. We used GNSS RO observation for these analyses as the dataset resolves the relevant features to provide information on the stratosphere–troposphere coupling.

In conclusion, our findings underscore the applicability of GNSS RO for the exploration of atmospheric circulation dynamics. Due to its high vertical resolution, GNSS RO has the potential for studying the interplay between tropopause structure and wave activity propagation.

References:

Leroy, S. S., and J. G. Anderson (2007), Estimating Eliassen–Palm flux using COSMIC radio occultation, Geophys. Res. Lett., 34, L10810, doi:10.1029/2006GL028263

Scherllin-Pirscher, B., A. K. Steiner, and G. Kirchengast (2014) Deriving dynamics from GPS radio occultation: Three-dimensional wind fields for monitoring the climate. Geophys. Res. Lett., 41, 7367–7374, doi:10.1002/2014GL061524.

Scherllin-Pirscher, B., A. K. Steiner, G. Kirchengast, M. Schwärz, and S. S. Leroy (2017), The power of vertical geolocation of atmospheric profiles from GNSS radio occultation, J. Geophys. Res. Atmos., 122, 1595–1616, doi:10.1002/2016JD025902.

Verkhoglyadova, O., S. Leroy, and C. Ao (2014), Estimation of winds from GPS radio occultations, J. Atmos. Oceanic Technol., doi:10.1175/JTECH-D-14-00061.1.

Minor Comment:

Line 151: Kordera et al., 2016 define recovery at 50 hPa, however, the vertical line denoting recover appears to based on 10 hPa temperatures in Fig. 3a. Some explanation is needed.

The vertical line in Fig.3a shows exactly when the temperature at 50 hPa is at its maximum.

Recommendation: Publish after address the two weaknesses noted above.

Thank you.

References:

Leroy, S. S., and Anderson, J. G.: Estimating Eliassen–Palm flux using COSMIC radio occultation, Geophys. Res. Lett., 34, L10810, doi:10.1029/2006GL028263, 2007.

Scherllin-Pirscher, B., Steiner, A. K., and Kirchengast, G.: Deriving dynamics from GPS radio occultation: Three-dimensional wind fields for monitoring the climate, Geophys. Res. Lett., 41, 7367–7374, https://doi.org/10.1002/2014GL061524, 2014.

Scherllin-Pirscher, B., A. K. Steiner, G. Kirchengast, M. Schwärz, and S. S. Leroy (2017), The power of vertical geolocation of atmospheric profiles from GNSS radio occultation, J. Geophys. Res. Atmos., 122, 1595–1616, doi:10.1002/2016JD025902.

Jucker, M.: Scaling of Eliassen-Palm flux vectors, Atmos. Sci. Lett., 22, e1020, https://doi.org/10.1002/asl.1020, 2021.

*Figure S4 from Supplementary Information

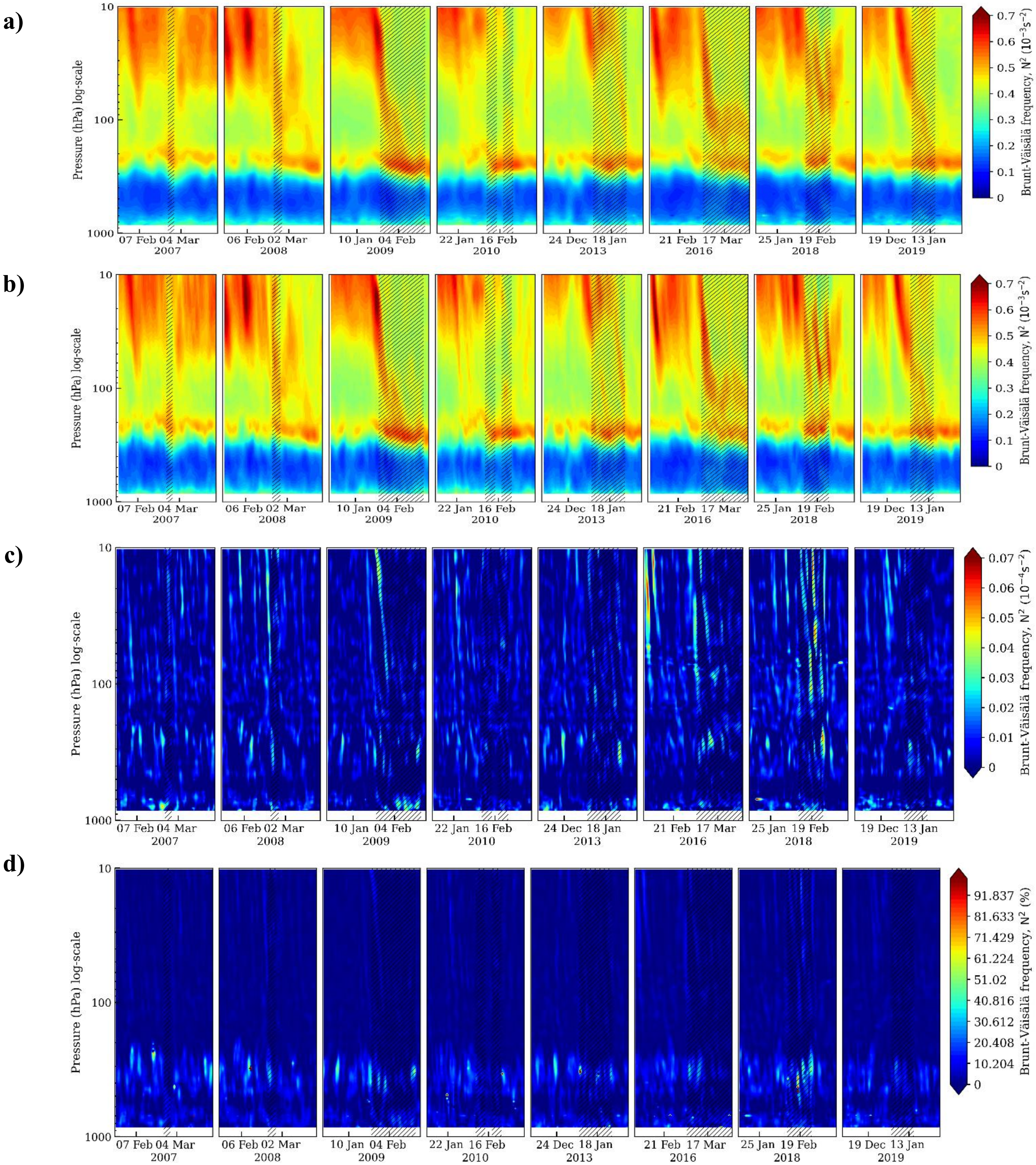

Figure S4. Brunt Väisälä frequency computed from RO (a) and ERA5 (b) and their difference (c) and difference in percentage (d) averaged over 75-90° N within a +/- 30 day

timeframe relative to each of the SSW events from 2007 to 2019. Hatched regions indicate dates when the zonal-mean zonal wind at 60° N and 10 hPa is negative.